This article has been accepted for publication in a future issue of this journal, but has not been fully edited. Content may change prior to final publication. Citation information: DOI 10.1109/TPEL.2014.2360404, IEEE Transactions on Power Electronics

Hybrid-type Full-bridge DC/DC Converter with High Efficiency

Sung-Ho Lee, Chun-Yoon Park, Jung-Min Kwon, *Member*, *IEEE*, and Bong-Hwan Kwon, *Member*, *IEEE*

***Abstract*— This paper presents a hybrid-type full-bridge dc/dc converter with high efficiency. Using a hybrid control scheme with a simple circuit structure, the proposed dc/dc converter has a hybrid operation mode. Under a normal input range, the proposed converter operates as a phase-shift full-bridge series-resonant converter that provides high efficiency by applying soft switching on all switches and rectifier diodes and reducing conduction losses. When the input is lower than the normal input range, the converter operates as an active-clamp step-up converter that enhances an operation range. Due to the hybrid operation, the proposed converter operates with larger phase-shift value than the conventional converters under the normal input range. Thus, the proposed converter is capable of being designed to give high power conversion efficiency and its operation range is extended. A 1kW prototype is implemented to confirm the theoretical analysis and validity of the proposed converter.**

***Index Terms*— Full-bridge circuit, phase-shift control, active-clamp circuit.**

I. INTRODUCTION

Nowadays, demands on dc/dc converters with a high power density, high efficiency, and low electromagnetic interference (EMI) have been increased in various industrial fields. As the switching frequency increases to obtain high power density, switching losses related to the turn-on and turn-off of the switching devices increase. Because these losses limit the increase of the switching frequency, soft switching techniques are indispensable.

Among previous dc/dc converters, a phase-shift full-bridge (PSFB) converter is attractive because all primary switches are turned on with zero-voltage switching (ZVS) without additional auxiliary circuits [1]. However, the PSFB converter has some serious problems such as narrow ZVS range of lagging-leg switches, high power losses by circulating current, and voltage ringing across rectifier diodes. Especially, with a requirement of wide input range, the PSFB converter is designed to operate with small phase-shift value under the normal input range; the design of the PSFB converter lengthens the freewheeling interval and causes the excessive circulating current which increases conduction losses [2], [3].

Recently, the various PSFB converters using auxiliary circuits have been introduced [4]-[12]. The PSFB converters extend ZVS range or reduce the circulating current by utilizing additional passive or active auxiliary circuits. However, the additional circuits result in complicated circuit configuration, complex control strategy, and extra power losses [13]. In addition, some PSFB converters still require the extra snubber to prevent serious voltage ringing problem across rectifier diodes. In [14], [15], the PSFB converters employing a series-resonant converter have been introduced, namely, the PSFB series-resonant converters; they have many advantages such as soft switching techniques of all primary switches and rectifier diodes, elimination of circulating current, reduction of voltage stress on rectifier diodes, and a simple circuit structure. However, when all aforementioned PSFB converters are required to guarantee a wide operation range, they still operate with the small phase-shift value under the normal input range. The operation with the small phase-shift value generally gives high conduction losses by high peak current; it results in low power efficiency. To achieve high efficiency under the normal input range and cover the wide input range, the different techniques are suggested. The converters in [16], [17] change the turn ratio of the transformer by using additional switching devices. Although the approach achieves high efficiency and ensures the wide input range, these techniques give circuit complexity and reduction of the transformer utilization.

Active-clamp circuits have been commonly used to absorb surge energy stored in leakage inductance of a transformer. Moreover, the circuits provide a soft switching technique [18], [19]. Some studies have introduced dc/dc converters combining the active-clamp circuit and voltage doubler or mulitpler rectifier [20], [21]. The circuit configuration allows to achieve a step-up function like a boost converter. The voltage stresses of rectifier diodes are also clamped at the output voltage and no extra snubber circuit is required.

In this paper, a novel hybrid-type FB dc/dc converter with high efficiency is proposed; the converter is derived from a combination of a PSFB series-resonant converter and an active-clamp step-up converter with a voltage doubler circuit. Using a hybrid control scheme with a simple circuit structure, the proposed converter has two operation modes. Under the normal input range, the proposed converter operates as a PSFB series-resonant converter. The proposed converter yields high efficiency by applying soft switching techniques on all the primary switches and rectifier diodes and by reducing conduction losses. When the input voltage is lower than the normal input range, the converter operates as an active-clamp step-up converter. In this mode, the proposed converter provides a step-up function by using

Manuscript received March 25, 2014; revised July 27, 2014.

This article has been accepted for publication in a future issue of this journal, but has not been fully edited. Content may change prior to final publication. Citation information: DOI 10.1109/TPEL.2014.2360404, IEEE Transactions on Power Electronics

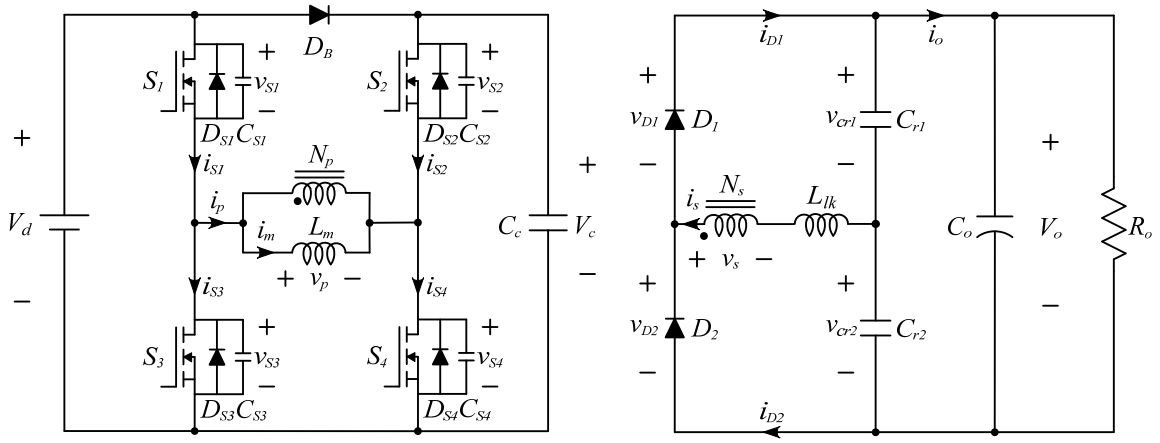

Fig. 1. Circuit diagram of the proposed hybrid-type full-bridge dc/dc converter.

the active-clamp circuit on the primary side and the voltage doubler rectifier on the secondary side. Due to the hybrid operation, the proposed converter operates with larger phase-shift value than the conventional PSFB converters under the normal input range. Thus, the proposed converter has the following advantages:

1) Under the normal input range, the proposed converter can be designed to optimize power conversion efficiency.
2) When the input is lower than the normal input range, the proposed converter performs a step-up function, which enhances the operation range.
3) Without complex circuit structures, the converter has high efficiency under the normal input range and extends the operation range.

The principle operation of the proposed converter is represented in Section II. The relevant analysis is given in Section III. Finally, a 1kW prototype of the proposed converter is implemented to confirm its theoretical analysis and validity.

II. Principle Operation of The Proposed Converter

Fig.1 shows a circuit diagram of the proposed converter. On the primary side of the power transformer T, the proposed converter has a FB circuit with one blocking diode D_B and one clamp capacitor C_c. On the secondary side, there is a voltage doubler rectifier. The operation of the proposed converter can be classified into two cases. The one is a PSFB series-resonant converter mode and the other is an active-clamp step-up converter mode.

To analyze the steady-state operation of the proposed converter, several assumptions are made.

1) All switches S_1, S_2, S_3, and S_4 are considered as ideal switches except for their body diodes and output capacitors.
2) The clamp capacitor C_c and output capacitor C_o are large enough, so the clamp capacitor voltage V_c and output voltage V_o have no ripple voltage, respectively.
3) The transformer T is composed of an ideal transformer with the primary winding turns N_p, the secondary winding turns N_s, the magnetizing inductance L_m, and the leakage inductance L_{lk}.
4) The capacitance of the resonant capacitors C_{r1} and C_{r2} is identical. Thus, C_{r1}=C_{r2}.

A. PSFB Series-resonant Converter Mode

Under the normal input voltage range, the proposed converter is operated by phase-shift control. In this mode, V_c is the same as the input voltage V_d and D_B is conducted. All switches are driven with a constant duty ratio 0.5 and short dead time. Fig. 2 and 3 show the operation waveforms and equivalent circuits, respectively. A detailed mode analysis is given as four modes.

Mode 1 [t_0, t_1]: Prior to t_0, the switches S_1 and S_2 are in on-state and the secondary current i_s is zero. The primary current i_p flows through D_B, S_1, S_2, and L_m. During this mode, the primary voltage v_p and secondary voltage v_s of the transformer T are zero. Thus, the magnetizing current i_m is constant and satisfies as follows:

$$i_m(t) = i_p(t) = i_m(t_0). \tag{1}$$

Mode 2 [t_1, t_2]: At t_1, S_2 is turned off. Because i_p flowing through S_2 is very low, S_2 is turned off with near zero-current. In this mode, i_p charges C_{S2} and discharges C_{S4}.

Mode 3 [t_2, t_3]: At t_2, the voltage across S_4 reaches zero. At the same time, i_p flows through the body diode D_{S4}. Thus, S_4 is turned on with zero-voltage while D_{S4} is conducted. In this mode, v_s is nV_d where the turn ratio n of the transformer is given by N_s/N_p and the secondary current i_s begins to flow through D_1. The state equation of this mode is written as follows:

$$L_{lk}\frac{di_s(t)}{dt} = nV_d - v_{cr1}(t) \tag{2}$$

$$i_s(t) = C_{r1}\frac{dv_{cr1}(t)}{dt} - C_{r2}\frac{dv_{cr2}(t)}{dt} \tag{3}$$

where v_{cr1} and v_{cr2} are the voltages across C_{r1} and C_{r2}, respectively. Since V_o is constant, the secondary current i_s can be obtained as

This article has been accepted for publication in a future issue of this journal, but has not been fully edited. Content may change prior to final publication. Citation information: DOI 10.1109/TPEL.2014.2360404, IEEE Transactions on Power Electronics

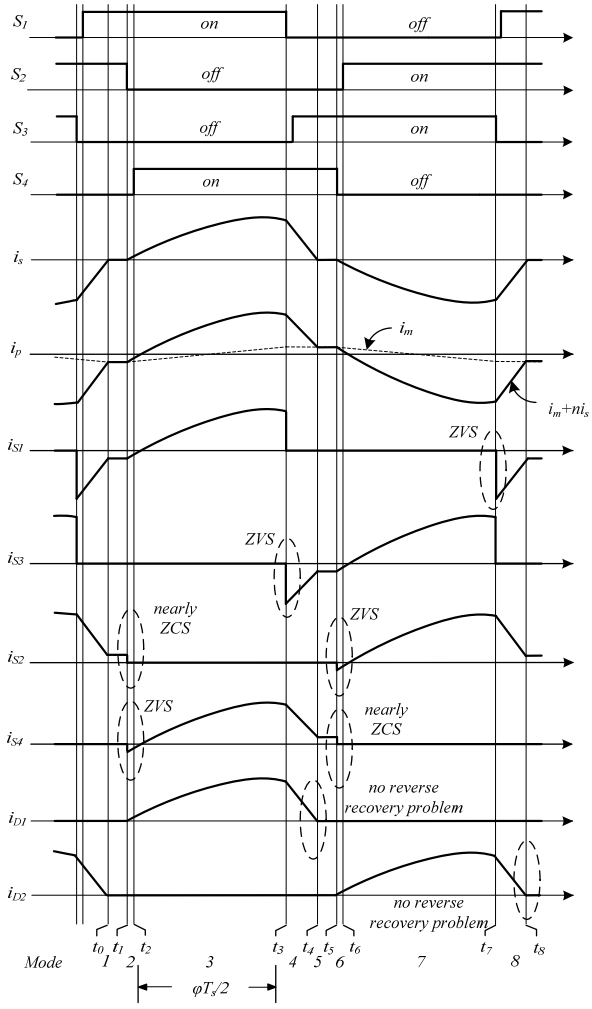

Fig. 2. Operation waveforms in the PSFB series-resonant converter mode.

$$i_s(t) = C_{r1}\frac{dv_{cr1}(t)}{dt} - C_{r2}\frac{d(V_o - v_{cr1}(t))}{dt} = C_r\frac{dv_{cr1}(t)}{dt} \tag{4}$$

where the equivalent resonant capacitance C_r is C_{r1}+C_{r2}. Using Eqns. (2) and (4), the secondary current i_s can be calculated as

$$i_s(t) = \frac{nV_d - v_{cr1}(t_2)}{Z_r}\sin\omega_r(t-t_2). \tag{5}$$

The angular frequency ω_r and characteristic impedance Z_r are given by

$$\omega_r = \frac{1}{\sqrt{L_{lk}C_r}}, \quad Z_r = \sqrt{\frac{L_{lk}}{C_r}}. \tag{6}$$

Meanwhile, the magnetizing current i_m increases linearly as follows:

$$i_m(t) = i_m(t_2) + \frac{V_d}{L_m}(t-t_2). \tag{7}$$

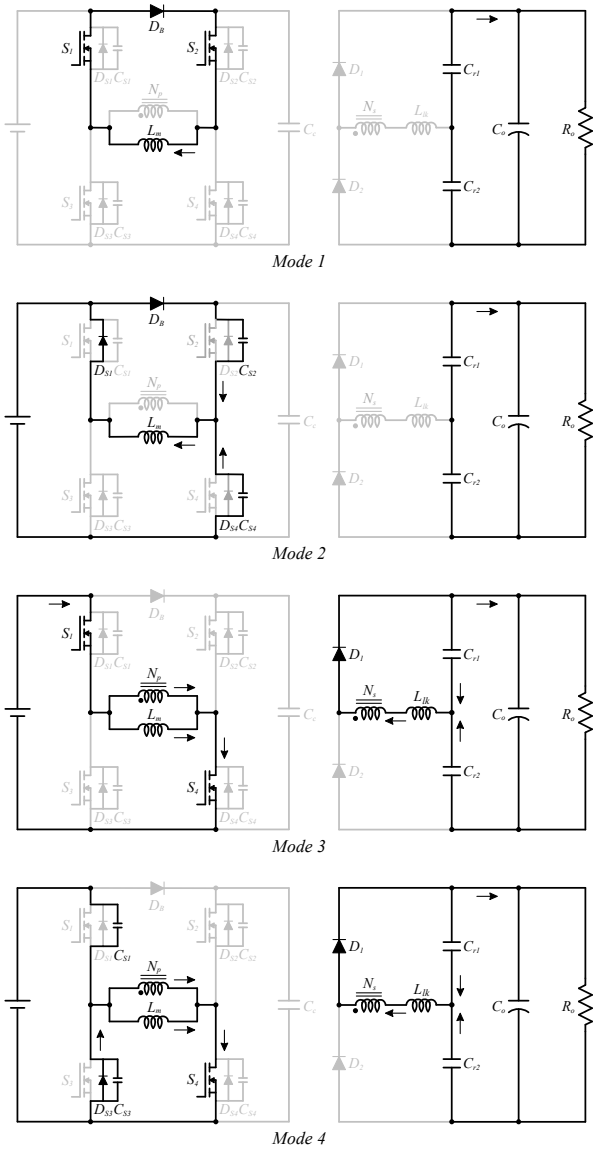

Fig. 3. Equivalent circuits during half period in the PSFB series-resonant converter mode.

In this mode, power is transferred from the input to the output.

Mode 4 [t_3, t_4]: This mode begins when S_1 is turned off. The primary current i_p charges C_{S1} and discharges C_{S3}. When the voltage across S_3 becomes zero, i_p flows through the body diode D_{S3}. Thus, S_3 is turned on with zero-voltage while D_{S3} is conducted. When v_p is zero, D_1 is still conducted and -v_{cr1} is applied to L_{lk}. Thus, the secondary current i_s goes to zero rapidly. End of this mode, since the secondary current is close to zero before D_1 is reverse bias, the losses by the reverse recovery problem are small as negligible.

Since operations during the next half switching period are similar with *Mode 1-4*, explanations of *Mode 5-8* are not presented.

B. Active-clamp Step-up Converter Mode

As the input voltage decreases up to a certain minimum value of the normal input range, the phase-shift value φ increases up to its maximum value, 1. If the input voltage is

This article has been accepted for publication in a future issue of this journal, but has not been fully edited. Content may change prior to final publication. Citation information: DOI 10.1109/TPEL.2014.2360404, IEEE Transactions on Power Electronics

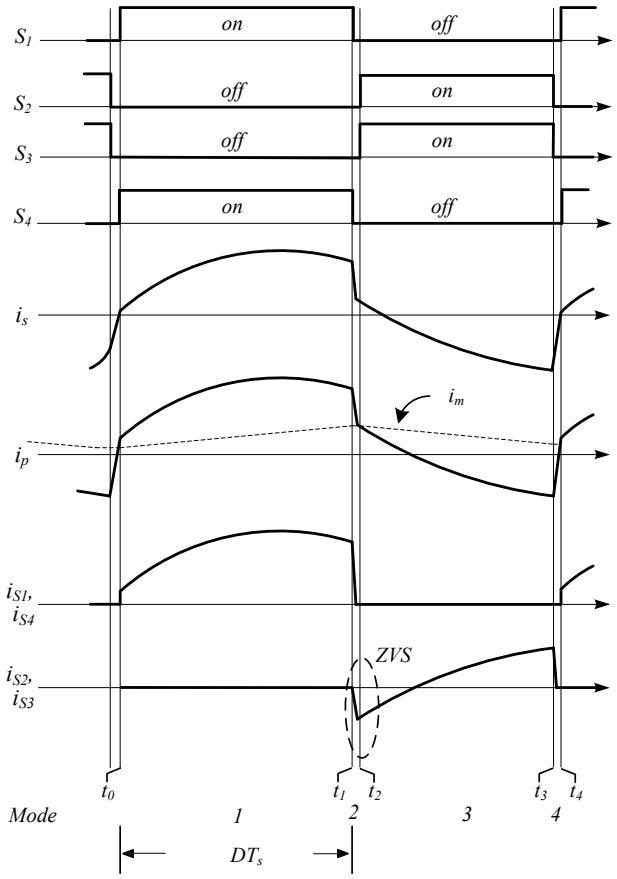

Fig. 4. Operation waveforms in the active-clamp step-up converter mode.

lower than the minimum value of the normal input range, the proposed converter is operated by dual asymmetrical pulse width modulation (PWM) control. The switches (S_1, S_4) and (S_2, S_3) are treated as switch pairs and operated complementarily with short dead time. The duty D over 0.5 is based on (S_1, S_4) pair. In this situation, the clamp capacitor voltage V_c is higher than V_d. Then, the blocking diode D_B is reverse biased and the proposed converter operates as the active-clamp step-up converter. Fig. 4 and 5 show the operation waveforms and equivalent circuits in the active-clamp step-up converter mode, respectively.

Mode 1 [t_0, t_1]: At t_0, S_1 and S_4 are turned on. Since V_d is applied to L_m, the magnetizing current i_m is linearly increased and is expressed as

$$i_m(t) = i_m(t_0) + \frac{V_d}{L_m}(t - t_0). \tag{8}$$

D_1 is conducted and the secondary current i_s begins to resonate by L_{lk}, C_{r1}, and C_{r2}. In this mode, the state equation is written as follows:

$$L_{lk}\frac{di_s(t)}{dt} = nV_d - v_{cr1}(t) \tag{9}$$

$$i_s(t) = C_{r1}\frac{dv_{cr1}(t)}{dt} - C_{r2}\frac{dv_{cr2}(t)}{dt} = C_r\frac{dv_{cr1}(t)}{dt}. \tag{10}$$

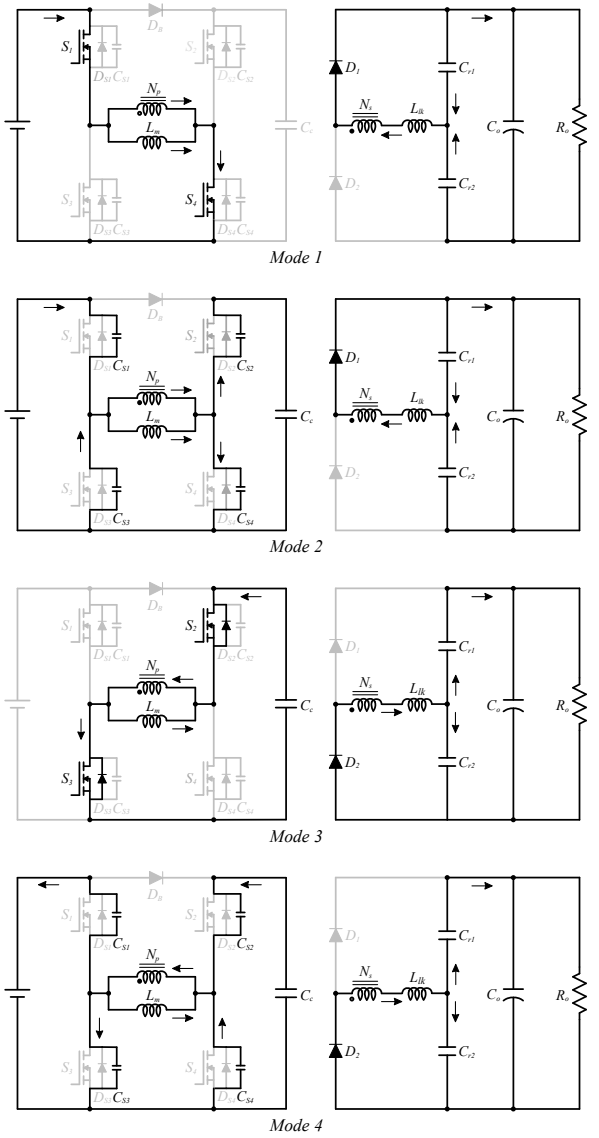

Fig. 5. Equivalent circuits during a switching period in the active-clamp step-up converter mode.

From Eqns. (9) and (10), the secondary current i_s can be calculated as

$$i_s(t) = i_s(t_3)\cos\omega_r(t - t_3) - \frac{nV_c - v_{cr2}(t_3)}{Z_r}\sin\omega_r(t - t_3). \tag{11}$$

In this mode, power is transferred from the input to the output.

Mode 2 [t_1, t_2]: At t_1, S_1 and S_4 are turned off. The primary current i_p charges and discharges the output capacitors of the switches during very short time.

Mode 3 [t_2, t_3]: This mode begins when the voltages across S_2 and S_3 are zero. At the same time, i_p flows through D_{S2} and D_{S3}. Thus, S_2 and S_3 are turned on with zero-voltage. Since the negative voltage -V_c is applied to L_m, the magnetizing current i_m decreases linearly as

$$i_m(t) = i_m(t_3) - \frac{V_c}{L_m}(t - t_3). \tag{12}$$

This article has been accepted for publication in a future issue of this journal, but has not been fully edited. Content may change prior to final publication. Citation information: DOI 10.1109/TPEL.2014.2360404, IEEE Transactions on Power Electronics

In this mode, the secondary current i_s begins to second resonance and the state equation is written as follows:

$$L_{lk}\frac{di_s}{dt} = v_{cr2}(t) - nV_c \tag{13}$$

$$i_s(t) = C_{r1}\frac{dv_{cr1}(t)}{dt} - C_{r2}\frac{dv_{cr2}(t)}{dt} = -C_r\frac{dv_{cr2}(t)}{dt}. \tag{14}$$

Using Eqns. (13) and (14), the secondary current is given by

$$i_s(t) = i_s(t_3)\cos\omega_r(t-t_3) - \frac{nV_c - v_{cr2}(t_3)}{Z_r}\sin\omega_r(t-t_3). \tag{15}$$

Mode 4 [t_3, t_4]: At t_3, S_2 and S_3 are turned off. The primary current i_p charges C_{S2}, C_{S3} and discharges C_{S1}, C_{S4} during very short time.

III. Analysis of The Proposed Converter

In the PSFB series-resonant converter mode, *Mode 4* is neglected since the duration of *Mode 4* is relatively very short. During *Mode 3*, the secondary current i_s in Eqn. (5) flows through D_1; the current is the same as sum of the current charging C_{r1} and current discharging C_{r2}. As shown in Fig.3, during the half switching period $T_s/2$, C_{r2} is discharged as much as the load current i_o while C_{r1} is charged. Thus, the average value of the current flowing through D_1 is the same as twice the load current during $T_s/2$. Due to the symmetric operation, the average value of the current flowing through D_2 is also twice the load current during the next half switching period. Both average values of v_{cr1} and v_{cr2} are $V_o/2$ and $v_{cr1}(t_2)$ in Eqn. (5) is obtained from the ripple voltage Δv_{cr1} of C_{r1} as

$$\begin{aligned} v_{cr1}(t_2) &= \frac{V_o}{2} - \frac{\Delta v_{cr1}}{2} = \frac{V_o}{2} - \frac{1}{2C_{r1}}\int i_{cr1}(\tau)d\tau \\ &= \frac{V_o}{2}\left(1 - \frac{T_s}{2C_{r1}R_o}\right) = \frac{V_o}{2}\left(1 - \frac{\pi Q}{2F}\right) \end{aligned} \tag{16}$$

where the frequency ratio F and quality factor Q are given by

$$F = \frac{f_s}{f_r}, \quad Q = \frac{4\omega_r L_{lk}}{R_o} = \frac{4}{\omega_r C_r R_o}. \tag{17}$$

Because the average value of the current flowing through D_1 during $T_s/2$ is the same as $2i_o$ and is zero during next half switching period, the average value of the current flowing through D_1 during T_s is equal to i_o. Thus, the load current i_o can be derived as

$$\begin{aligned} i_o &= \frac{V_o}{R_o} = \frac{1}{T_s}\left[\int_{t_2}^{t_2+\varphi T_s/2}\frac{nV_d - v_{cr1}(t_2)}{Z_r}\sin\omega_r(\tau - t_2)d\tau\right] \\ &= F\left[\frac{nV_d - v_{cr1}(t_2)}{2\pi Z_r}(1-\cos\frac{\pi\varphi}{F})\right]. \end{aligned} \tag{18}$$

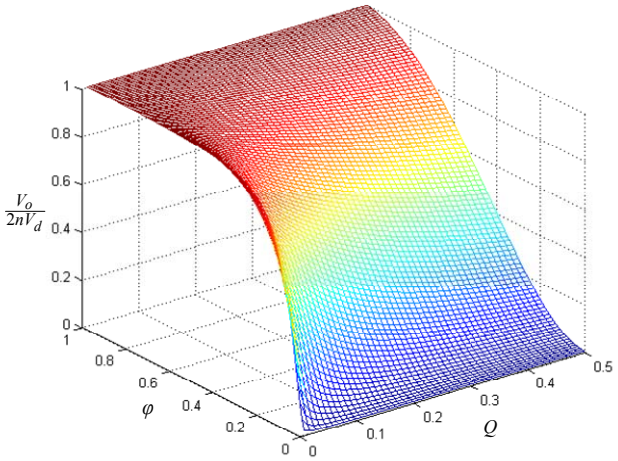

Fig. 6. Normalized voltage gain at F=1.05 in the PSFB series-resonant converter mode.

From Eqns. (16) and (18), the voltage gain in the PSFB series-resonant converter mode can be derived as follows:

$$\frac{V_o}{V_d} = \frac{2n}{\frac{\pi Q}{F(1-\cos\frac{\pi\varphi}{F})} + \left(1 - \frac{\pi Q}{2F}\right)}. \tag{19}$$

Fig. 6 shows the normalized voltage gain in the PSFB series-resonant converter mode.

In the active-clamp step-up converter mode, the average voltage V_c for $D > 0.5$ is obtained as

$$V_c = \frac{D}{1-D}V_d. \tag{20}$$

By the volt-second balance law for the magnetizing inductance L_m, the following equations are derived as

$$nV_d DT_s = \frac{n^2 L_m}{n^2 L_m + L_{lk}}V_{cr2}(1-D)T_s \tag{21}$$

$$\frac{n^2 L_m}{n^2 L_m + L_{lk}}V_{cr1}DT_s = nV_c(1-D)T_s \tag{22}$$

where V_{cr1} and V_{cr2} are the average values of the voltages across C_{cr1} and C_{cr2}, respectively. The sum of V_{cr1} and V_{cr2} is V_o. From Eqns. (21) and (22), the average values V_{cr1} and V_{cr2} are obtained as

$$V_{cr1} = \frac{n^2 L_m + L_{lk}}{nL_m}V_d = (1-D)V_o \tag{23}$$

$$V_{cr2} = \frac{n^2 L_m + L_{lk}}{nL_m}\frac{D}{1-D}V_d = DV_o. \tag{24}$$

Assuming L_{lk} is much smaller than L_m, the voltage gain in the active-clamp step-up converter mode can be derived as follows:

This article has been accepted for publication in a future issue of this journal, but has not been fully edited. Content may change prior to final publication. Citation information: DOI 10.1109/TPEL.2014.2360404, IEEE Transactions on Power Electronics

$$\frac{V_o}{V_d} = \frac{n}{1-D}. \tag{25}$$

The voltage gain becomes that of an isolated boost converter. It means that the proposed converter performs step-up function in the active-clamp step-up converter mode.

In the PSFB series-resonant converter, the leading-leg switches S_1 and S_3 can be easily turned on with zero-voltage by the reflected secondary current. However, when the state of the lagging-leg switches S_2 and S_4 are changed, the secondary current is zero. Thus, only the energy stored in L_m is involved in ZVS of the lagging-leg switches condition; it is obtained as

$$\frac{1}{2}L_m\left(\frac{\Delta i_m}{2}\right)^2 = \frac{1}{2}L_m\left(\frac{\varphi V_d}{4L_m f_s}\right)^2 > \frac{4}{3}C_m V_d^2 \tag{26}$$

where C_m is the output capacitance of the MOSFET switches. From Eqn. (26), the magnetizing inductance L_m can be decided as

$$L_m < \frac{3\varphi_{\min}^2}{128 C_m f_s^2} \tag{27}$$

where φ_{min} is the minimum value of φ. The ZCS condition of the lagging-leg switches is related to the frequency ratio. As F increases, the ZCS range decreases [15]. Therefore, to guarantee both ZVS of all primary switches and ZCS of the lagging-leg switches, F should be selected to be slightly more than one. In the active-clamp step-up converter mode, S_2 and S_3 can achieve ZVS turn-on naturally from the asymmetrical PWM operation.

As shown in Fig.2, in the PSFB series-resonant converter mode, L_{lk} performs as the output inductor and all energy stored in L_{lk} is delivered to the load until the secondary current is zero. Then, only small magnetizing current flows on the primary side. In the active-clamp step-up converter, the proposed converter is operated by dual asymmetrical PWM control scheme. In the PWM scheme, there is no circulating current [22]. Thus, the proposed converter eliminates the conduction loss by the circulating current in the entire operation range.

IV. Implementation and Experiments

To evaluate a feasibility of the proposed converter, a 1kW prototype was built and tested. The operation range of the proposed converter is from 250V to 350V. The output voltage is designated as 200V and the normal input range is set up from 320V to 350V.

A. Implementation of The Prototype

Considering power conversion efficiency under the normal input range, the proposed converter is designed. To obtain ZVS turn-on of the switches, the switching frequency f_s should be higher than the resonant frequency f_r. By the design rule proved in [15], the frequency ratio F (f_s/f_r) is selected to be slightly more than one. The quality factor Q is decided by Eqn. (17). If Q is too small, the proposed converter is operated with small φ under the normal input range. Thus, L_{lk} is selected as 8.3μH. From the normal input range, the turn ratio n is decided by Eqn. (19) and Fig. 6. All switch stresses are determined by

TABLE I
PARAMETERS OF THE PROTOTYPE

Parameters	Symbols	Value
Input voltage	V_d	250-350V
Output voltage	V_o	200V
Switching frequency	f_s	50kHz
Primary winding turns	N_p	24turns
Secondary winding turns	N_s	8turns
Magnetizing inductance	L_m	695μH
Leakage inductance	L_{lk}	8.3μH
Clamp capacitor	C_c	11μF
Resonant capacitors	C_{r1},C_{r2}	680nF
Output capacitor	C_o	680μF
Switches	S_1, S_2, S_3, S_4	STW26NM60
Blocking diode	D_B	FFAF40U60DN
Output diodes	D_1, D_2	FFPF15U40S

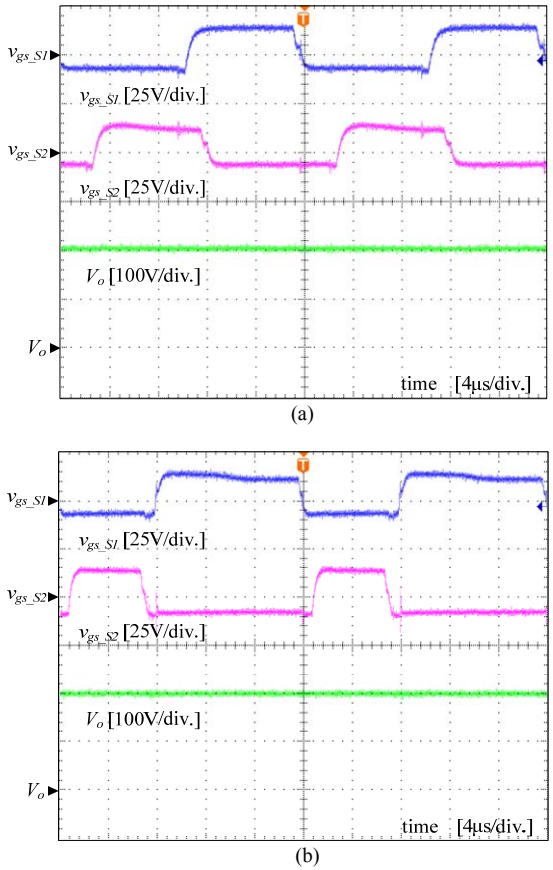

Fig. 7. Experimental waveforms for the gate signals and output voltage according to the operation mode. (a) PSFB series-resonant converter mode when V_d=350V. (b) Active-clamp step-up converter when V_d=250V.

This article has been accepted for publication in a future issue of this journal, but has not been fully edited. Content may change prior to final publication. Citation information: DOI 10.1109/TPEL.2014.2360404, IEEE Transactions on Power Electronics

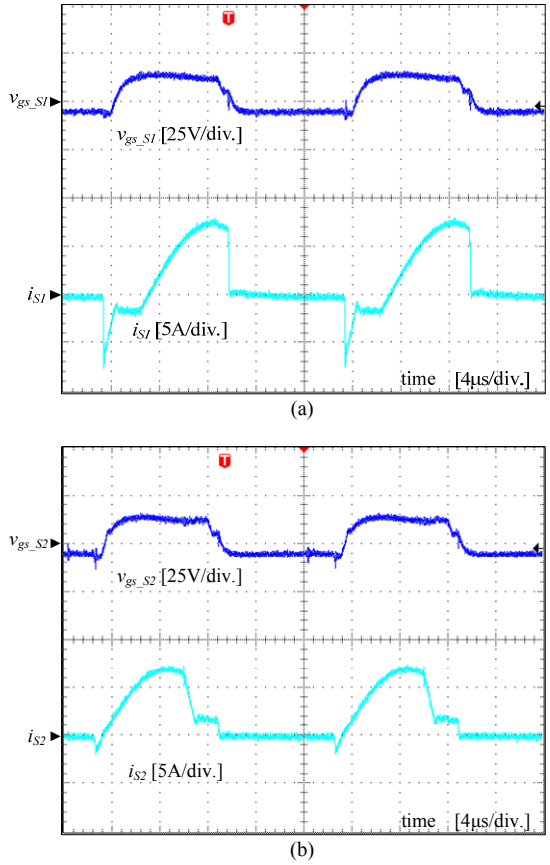

Fig. 8. Experimental waveforms for soft switching in the PSFB series-resonant converter mode. (a) ZVS turn-on of S_1. (b) ZVS turn-on and ZCS turn-off of S_2.

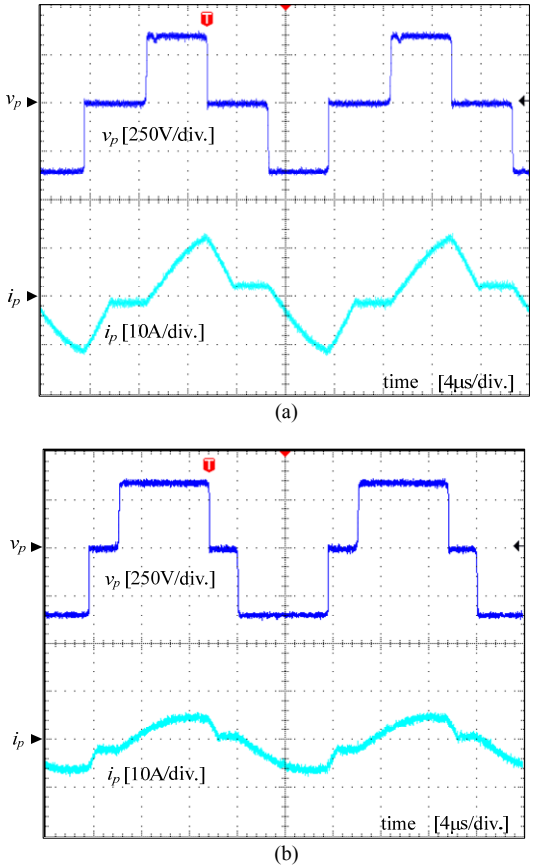

Fig. 9. Experimental waveforms for the current stress when V_d=350V. (a) Conventional PSFB series-resonant converter. (b) Proposed converter.

the input voltage in the PSFB series-resonant converter mode. On the other hand, in the active-clamp step-up converter mode, the voltage stress of the switches S_1 and S_2 are the same as the input voltage and those of S_3 and S_4 are determined by Eqn. (20). In both the operation modes, voltage stresses of the rectifier diodes are clamped at the output voltage V_o. The major experimental parameters are presented in Table I. The prototype is implemented using a single DSP chip, dsPIC33EP512GM604 (Microchip) which provides both phase-shift and asymmetrical PWM control.

B. Experimental Results

Fig. 7 shows waveforms for the gate signals and output voltage in the proposed converter according to the operation mode. v_{gs_S1} and v_{gs_S2} are each gate signal for S_1 and S_2, respectively. When the input voltage is 350V, the proposed converter is operated by phase-shift control with the constant duty 0.5. On the other hand, when the input voltage is 250V, the proposed converter is operated by the asymmetrical PWM control with the duty 0.61. In both operation modes, the proposed converter regulates v_o. Fig. 8 (a) and (b) show waveforms for the gate signals and currents of S_1 and S_2 at full load condition when V_d = 350V. When the switches are turned on, the currents flow through the body diode of each switch. It is clear that all switches are turned on with zero-voltage. Furthermore, as shown in Fig. 8 (b), S_2 is turned off with near

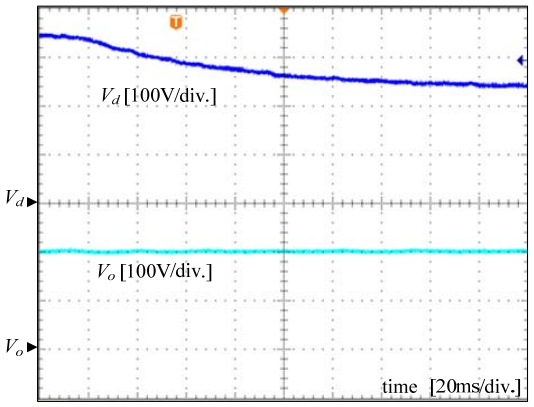

Fig. 10. Experimental waveforms for the input voltage V_d and output voltage V_o in the transition-state.

zero current as the theoretical analysis. Fig. 9 show waveforms for the primary voltage v_p and current i_p of the conventional PSFB series-resonant converter and the proposed converter at full-load condition under the normal input range. In the conventional PSFB series-resonant converter, to guarantee the designated operation range, higher turn ratio n (=0.417) is required than the proposed converter. Other parameters are shown in Table I. When the input voltage V_d is 350V, the conventional converter operates with small φ (=0.5). On the other hand, the proposed converter is operated with larger φ

This article has been accepted for publication in a future issue of this journal, but has not been fully edited. Content may change prior to final publication. Citation information: DOI 10.1109/TPEL.2014.2360404, IEEE Transactions on Power Electronics

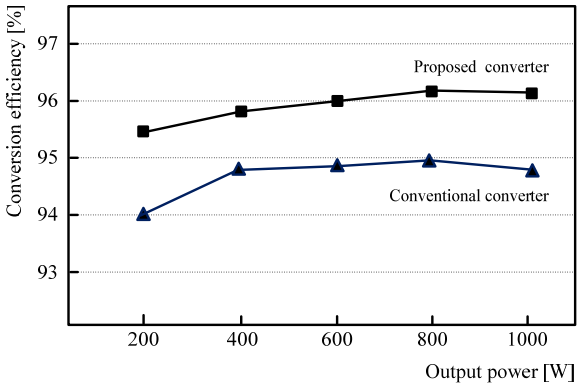

Fig. 11. Measured efficiencies under the normal input range according to the output power

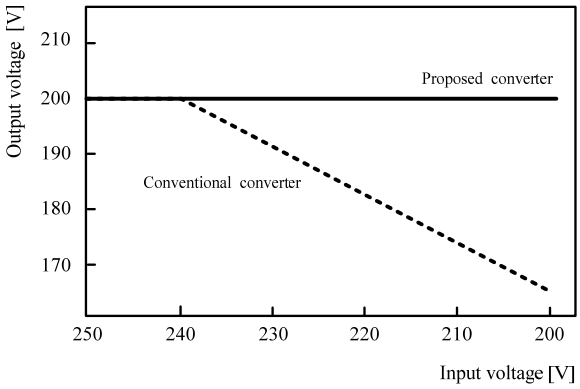

Fig. 12. Variation of output voltage in the below designated operation range.

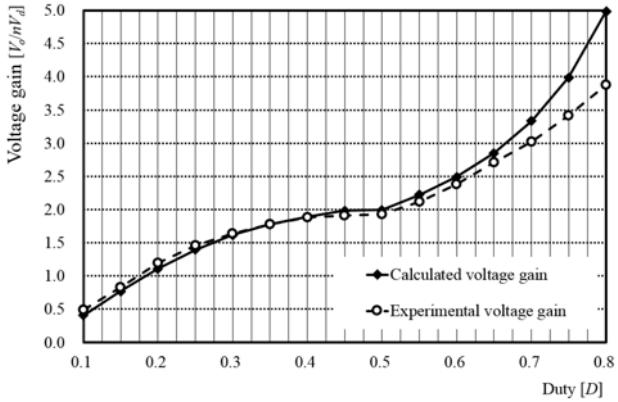

Fig. 13. Comparison between analytical and experimental voltage gain.

(=0.75). As shown in Fig. 9, the current stress in the proposed converter is much lower. In addition, the proposed converter eliminates the circulating current. Fig. 10 shows waveforms for the input and output voltages in the transient-state. When the input voltage V_d is reduced from 350V to 250V, the proposed converter regulates the output voltage without any hysteresis. Fig. 11 shows measured efficiencies for the conventional series-resonant converter and the proposed converter when V_d =350V. It shows that the proposed converter has higher efficiency over all load conditions. Fig. 12 shows the variation of the output voltage V_o at full-load condition when the input voltage V_d decreases from 250V to 200V. As shown in Fig. 12, in the below designated operation range of the conventional converter, V_o decreases. In the proposed converter, V_o is maintained as 200V although the input voltage decreases below the designated operation range. Fig. 13 shows the comparative plot of analytical and experimental voltage gain of the proposed converter. When the phase-shift value φ is expressed using the duty D, $\varphi/2$ can be represented as D. The measured voltage gain is similar to the theoretical analysis in Eqns. (19) and (25). As shown in the Fig. 13, the proposed converter has both the step-down and step-up functions.

V. Conclusion

The novel hybrid-type full-bridge dc/dc converter with high efficiency has been introduced and verified by the analysis and experimental results. By using the hybrid control scheme with the simple circuit structure, the proposed converter has both the step-down and step-up functions, which ensure to cover the wide input range. Under the normal input range, the proposed converter achieves high efficiency by providing soft switching technique to all the switches and rectifier diodes, and reducing the current stress. When the input is lower than the normal input range, the proposed converter provides the step-up function by using the active-clamp circuit and voltage doubler, which extends the operation range. To confirm the validity of the proposed converter, 1kW prototype was built and tested. Under the normal input range, the conversion efficiency is over 96% at full-load condition, and the input range from 250V to 350V is guaranteed. Thus, the proposed converter has many advantages such as high efficiency and wide input range.

References

[1] J. A. sabaté, V.Vlatkovic, R. B. Ridley, F. C. Lee, and B. H. Cho, "Design considerations for high–voltage high-power full-bridge zero-voltage- switching PWM converter," in *Proc. Appl. Power Electron. Conf.*, 1990, pp. 275-284.

[2] I. O. Lee and G. W. Moon, "Phase-shifted PWM converter with a wide ZVS range and reduced circulating current," *IEEE Trans. Power Electron.*, vol. 28, no .2, pp. 908-919.Feb. 2013

[3] Y. S. Shin, S. S. Hong, D. J. Kim, D. S. Oh, and S. K. Han, "A new changeable full bridge dc/dc converter for wide input voltage range," in Proc. *8th Int. Conf. Power Electron.-ECCE Asia*, May 2011, pp. 2328-2335.

[4] P. K. Jain, W., Kang, H. Soin, Y., Xi, "Analysis and design considerations of a load and line independent zero voltage switching full bridge dc/dc converter topology," *IEEE Trans. Power Electron.*, vol. 17, no .5, pp. 649-657.Sep. 2002

[5] I. O. Lee and G. W. Moon, "Soft-switching DC/DC converter with a full ZVS range and reduced output filter for high-voltage application," *IEEE Trans. Power Electron.*, vol. 28, no .1, pp. 112-122.Jan. 2013

[6] G. N. B. Yadav and N. L. Narasamma, "An active soft switched phase-shifted full-bridge dc-dc converter : analysis, modeling, design, and implementation," *IEEE Trans. Power Electron.*, vol. 29 no. 9, pp. 4538-4550, Sep. 2014.

[7] Y. Jang, M. M. Jovanović, and Y. –M. Chang, "A new ZVS-PWM full-bridge converter," *IEEE Trans. Power Electron.*, vol. 18 no. 5, pp. 1122-1129, Sep. 2003.

This article has been accepted for publication in a future issue of this journal, but has not been fully edited. Content may change prior to final publication. Citation information: DOI 10.1109/TPEL.2014.2360404, IEEE Transactions on Power Electronics

[8] T. T. Song and N. Huang, "A novel zero-voltage and zero-current-switching full-bridge PWM converter," *IEEE Trans*. *Power Electron*., vol. 20, no. 2, pp. 286-291, Mar. 2005.
[9] R. Huang and S. K. Mazumder, "A soft-switching scheme for an isolated dc/dc converter with pulsating dc output for a three-phase high-frequency link PWM converter," *IEEE Trans*. *Power Electron*., vol. 24, no. 10, pp. 2276-2288, Oct. 2009.
[10] K. W. Seok and B. H. Kwon, "An improved zero-voltage and zero-current-switching full-bridge PWM converter using a simple resonant circuit, " *IEEE Trans*. *Ind*. *Electron*., vol. 48 no. 6, pp. 1205-1209, Dec. 2001.
[11] M. Pahlevaninezhad, P. Das, J. Drobnik, P. K. Jain, and A. Bakhshai, "A novel ZVZCS full-bridge dc/dc converter used for electric vehicles," *IEEE Trans*. *Power Electron*., vol. 27, no. 6, pp. 2752-2769, Jun. 2012.
[12] J. Drobnik, M. Bodor, and M. Pastor, "Soft-switching full-bridge PWM dc-dc converter with controlled output rectifier and secondary energy recovery turn-off snubber," *IEEE Trans*. *Power Electron*., vol. 29, no. 8, pp. 4116-4125, Aug. 2014.
[13] B., Gu, J.-S. Lai, N. Kees, C. Zheng, "Hybrid-switching full-bridge dc–dc converter with minimal voltage stress of bridge rectifier, reduced circulating losses, and filter requirement for electric vehicle battery chargers," *IEEE Trans*. *Power Electron*., vol.28, no.3, pp.1132-1144, Mar. 2013.
[14] W. J. Lee, C. E. Kim, G. W. Moon, and S. K. Han, "A new phase-shifted full-bridge converter with voltage-doubler-type rectifier for high-efficiency PDP sustaining power module," *IEEE Trans*. *Ind*. *Electron*., vol. 55 no. 6, pp. 2450-2458, Jun. 2008.
[15] E. H. Kim and B. H. Kwon, "Zero-voltage-and zero-current-switching full-bridge converter with secondary resonance," *IEEE Trans*. *Ind*. *Electron*., vol. 57 no. 3, pp. 1017-1025, Mar. 2010.
[16] B. Yang, P. Xu, and F. C. Lee, "Range winding for wide input range front end dc/dc converter," in *Proc*. *IEEE Appl*. *Power Electron*. *Conf*., 2001, pp. 476-479.
[17] X. Wang, F. Tian, and I. Batarseh, "High efficiency parallel post regulator for wide range input dc-dc converter," *IEEE Trans*. *Power Electron*., vol. 23, no. 2, pp. 852-858, Mar. 2008.
[18] R. Watson, F. C. Lee, and G. C. Hua, "Utilization of an active-clamp circuit to achieve soft switching in flyback converters," *IEEE Trans*. *Power Electron*., vol. 11, no. 1, pp. 162-169, Jan. 1996.
[19] Q. Li, F. C. Lee, S. Buso, and M. M. Jovanovic, "Large-signal transient analysis of forward converter with active-clamp reset," *IEEE Trans*. *Power Electron*., vol. 17, no. 1, pp. 15-24, Jan. 2002.
[20] W. Y. Choi, "High-efficiency DC-DC converter with fast dynamic response for low voltage photovoltaic sources," *IEEE Trans*. *Power Electron*., vol. 28, no. 2, pp. 706-716, Feb. 2013.
[21] G. Spiazzi, P. Mattavelli, and A. Costabeber, "High step-up ratio flyback converter with active clamp and voltage multiplier," *IEEE Trans*. *Power Electron*., vol. 26, no. 11, pp. 3205-3214, Nov. 2011.
[22] P. Imbertson and N. Mohan, "Asymmetrical duty cycle permits zero switching loss in PWM circuits with no conduction loss penalty," *IEEE Trans*. *Ind*. *Appl*., vol. 29, no. 1, pp. 121-125, Jan. 1993.

Sung-Ho Lee was born in Seoul, Korea, in 1985. He received the B.S degree in electrical engineering from Dongguk University, Seoul, Korea, in 2011. He is currently working toward the Ph.D. degree in electronic and electrical engineering in Pohang University of Science and Technology, (POSTECH), Pohang, Korea. His research interests include dc-dc converters, grid-connected inverters, and renewable energy system.

Chun-Yoon Park was born in Yeongju, Korea, in 1984. He received the B.S. and Ph.D. degree in electronic and electrical engineering from Pohang University of Science and Technology, Pohang, Korea, in 2008 and 2014, respectively. He is currently a Senior Engineer in the Samsung Electronics Co., Ltd., Korea. His research interests are dc-dc converter, power-factor correction, and switch-mode power supplies.

Jung-Min Kwon (S'08, M'09) was born in Ulsan, Korea, in 1981. He received the B.S. degree in electrical and electronic engineering from Yonsei University, Seoul, Korea, in 2004, and the Ph.D. degree in electronic and electrical engineering from Pohang University of Science and Technology (POSTECH), Pohang, Korea, in 2009.

From 2009 to 2011, he has been with the Samsung Advanced Institute of Technology, Yongin, Korea. Since 2011, he has been with the Department of Electrical Engineering, Hanbat National University, Daejeon, Korea, where he is currently a Professor. His research interests include direct methanol fuel cell, renewable energy system, and distributed generation.

Bong-Hwan Kwon (M'91) was born in Pohang, Korea, in 1958. He received the B.S. degree from the Kyungpook National University, Deagu, Korea, in 1982 and the M.S. and Ph.D. degrees in electrical engineering from the Korea Advanced Institute of Science and Technology, Seoul, Korea, in 1984 and 1987, respectively.

Since 1987, he has been with the Department of Electronic and Electrical Engineering, Pohang University of Science and Technology (POSTECH), Pohang, Korea, where he is currently a Professor. His research interests include converters for renewable energy, high-frequency converters, and switch-mode power supplies.